

ARTICLE IN PRESS



Available online at www.sciencedirect.com



NEUROCOMPUTING

Neurocomputing III (IIII) III-III

www.elsevier.com/locate/neucom

1

An integrate-and-fire model of a cerebellar granule cell

3

Michele Bezzi^{a,*},¹ Thierry Nieuws^b, Olivier J.-M. Coenen^a,
Egidio D'Angelo^{b,2}

5

^aSONY CSL, F-75005, Paris, France

7

^bDepartment of Molecular/Cellular Physiology and University of Pavia, I-27100, Pavia, Italy

Abstract

9 We present a simple spiking model that extends the classical integrate-and-fire neuron to re-
10 produce the different dynamical behaviors observed in cerebellar granule cells. The model is two
11 dimensional: in addition to the membrane potential V , we consider a gating variable that models
12 a slow K^+ current. This current plays a major role in generating the rhythmic behavior and reso-
13 nance in the model. Despite its simplicity this model is able to reproduce most of the properties
14 observed in granule cell recordings and in numerical simulations with high-dimensional Hodgkin-
15 Huxley models.

© 2004 Published by Elsevier B.V.

17 *PACS:* 87.17.Nn; 87.17.Aa; 87.19.La

Keywords: Cerebellum; Integrate-and-fire neuron; Resonance

19 1. Introduction

21 The cerebellum is involved in many aspects of motor control and sensorimotor co-
22 ordination. The architecture of the cerebellar cortex is well defined and is composed
23 of three layers: the granular, molecular and Purkinje cells layer. The major afferents
24 to the cerebellum are the mossy fibers that carry sensory and neocortical informations
25 and that make synapses onto the granule cells in the input layer, the granular layer,
of the cerebellum. The cerebellar granular layer contains a large number of granule

* Corresponding author. Tel.: +33-1-44-08-05-18; fax: +33-1-45-87-87-50.

E-mail address: michele@csl.sony.fr (M. Bezzi).

¹ The first two authors contributed equally to this work.

² Also: Istituto Nazionale Fisica Della Materia, Pavia Unit.

1 cells (on the order of 10^{12} in humans, i.e., more than the overall number of neurons
2 in the cerebral cortex) and there are $\approx 10^3$ as many granule cells as mossy fibers.
3 The granule cells have been suggested to be involved in expansion recoding [8] that
4 would be used to decorrelate and build a sparse representation of mossy fibers inputs
5 for further processing in the molecular and Purkinje layers [1,8,10].

6 A granule cell represents the basic computational unit of the granular layer since
7 they receive the external inputs and transmit their output to the Purkinje cells. A clear
8 understanding of single-cell properties, as well as a biophysically reasonable model, yet
9 computationally simple, are needed before studying the behavior of the granular layer
10 network as a whole. A granule cell shows interesting responses even in rather simple
11 experimental conditions. Resonance and bursting behaviors have been observed in rat
12 cerebellar granule cells in patch-clamp recordings [4]. Oscillations and resonance are
13 suggested to arise from the interplay between a slow repolarizing potassium current
14 I_{K-SLOW} and fast persistent depolarizing sodium current I_{Na-p} . These conclusions are
15 supported by experimental studies as well as by a detailed Hodgkin–Huxley model of a
16 granule cell written in the NEURON simulation software [4]. This single-compartment
17 model is a set of 15 coupled differential equations that mimics the evolution of 10 dif-
18 ferent ionic currents, plus additional equations for intracellular calcium concentration
19 and for membrane potential. The model reproduces the time course of measured ionic
20 currents under different conditions, as well as oscillatory, resonance and bursting behav-
21 iors of granule cells. Even though these Hodgkin–Huxley-type models are biophysically
22 precise and can reproduce in great detail the dynamics of neurons, they are computa-
23 tionally inefficient for simulating large networks due to the large numbers of coupled
24 differential equations involved. In addition, they are often difficult to understand and
25 analyze due the presence of several coupled equations and parameters, and relatively
26 simple phenomena can be obscured by the complexity of the model. A possible strat-
27 egy is to use simpler models such as integrate-and-fire model [7]. An integrate-and-fire
28 neuron, in its simplest form, is a simple linear integrator with a threshold mechanism
29 for spike generation: When the membrane potential crosses a certain threshold, the
30 neuron spikes, and the potential is reset. Despite its simplicity it can generate very
31 realistic-looking spike trains. This basic integrate-and-fire neuron has been extend in to
32 model many interesting non-linear phenomena observed in neurons, such as oscillations
33 [9], resonance [5] and bursting [11].

34 We propose here a two-dimensional integrate-and-fire model for studying the be-
35 havior a single granule cell. Our simplified model can be directly related to the mul-
36 tidimensional model presented in [4] and mentioned above. Basically, the simplified
37 model is obtained by removing all the currents involved in spike generation, and con-
38 sidering the fast currents as instantaneous ones. This mapping helps the calibration of
39 the parameters that can be easily derived from the more detailed model, which in turn
40 is finely tuned to match the biophysical data. In our model we have considered the
41 following active currents: a fast sodium current I_{Na-p} , a fast inward rectifier current
42 I_{K-ir} and a slow potassium current I_{K-slow} . In addition, we have a passive leakage cur-
43 rent I_{Leak} and an external applied current I_{App} . The fast currents I_{Na-p} and I_{K-ir} have
44 relaxation times of the order of a few milliseconds. Therefore, compared to $\simeq 60$ ms
45 for I_{K-slow} , these fast currents can be considered instantaneous and we can replace the

1 kinetics of their gating functions with the corresponding steady state values ($a_\infty(V)$
 2 and $m_\infty(V)$, respectively). In addition, all the currents needed for spike generation
 3 are not explicitly considered, since we model it with a simple threshold process. The
 simplified neuron can be described by the two equations

$$C \frac{dV}{dt} = g_{K\text{-slow}} (V - V_K) n(V, t) + I_{\text{Active}} + I_{\text{Leak}} - I_{\text{App}},$$

$$\frac{dn}{dt} = \frac{n - n_\infty}{\tau_n},$$

5 where V is the potential across the membrane with a capacitance C , and

$$I_{\text{Active}} = g_{K\text{-ir}}(V - V_K) m_\infty(V) + g_{\text{Na-p}}(V - V_{\text{Na}}) a_\infty(V),$$

$$I_{\text{Leak}} = g_{\text{LeakA}}(V - V_{\text{LeakA}}) + g_{\text{GABA-A}}(V - V_{\text{GABA-A}}).$$

I_{Active} is the sum of active currents (for sake of clarity we have separated the con-
 7 tribution of $I_{K\text{-slow}} = g_{K\text{-slow}} (V - V_K) n(V, t)$ from this expression) and I_{Leak} is the
 contribution of the two leakage currents: non-specific and *GABA-A*. Finally, $n(V, t)$
 9 is the time-dependent gating variable that regulates $I_{K\text{-slow}}$ dynamics. This model still
 presents a large numbers of parameters (see Table 1); their number can be further
 11 reduced by introducing dimensionless parameters, such as measuring the conductance
 in C/τ unit, or by merging together the currents with no explicit dependence on time
 13 (i.e., I_{Active}) and, of course, replacing the two passive leakage resistors with the corre-
 sponding equivalent circuit. However, in order to keep clear the biological meaning of
 15 each parameter, in this paper we will keep all the equations in their original form. In
 Table 1, we show the parameter values used in all simulations, following Ref. [4],
 17 whose choices are based on experimental data. We tested our model with a variety
 of external inputs; following the experiments in [4], we will focus here on two differ-
 19 ent inputs: a current step and an sinusoidal current. In Fig. 1 we show the repetitive
 firing of the simplified model. We injected a strong depolarizing current step, 10 and
 21 20 pA in Fig. 1A and B respectively, the neuron starts firing regularly with a slight
 adaptation. The input–output relationship for the neuron is shown in Fig. 2A. The fre-
 23 quency increases linearly with the input current in a range of 8–32 pA. Below 8 pA,
 our neuron with the current set of parameters does not reach the spiking threshold, in
 25 agreement with experimental [1,2] and previous modeling (see Fig. 8A in Ref. [4])
 results. Decreasing the input current the neuron shows persistent sub-threshold oscilla-
 27 tions. Phase plane analysis, varying $g_{K\text{-slow}}$, shows that the mechanism for the onset of
 oscillations is an Hopf bifurcation (i.e., frequency at onset has a non-zero minimum),
 29 and in the oscillatory state, the corresponding period does not vary greatly with $g_{K\text{-slow}}$.
 Sub-threshold oscillatory phenomena can strongly affect the temporal coding capabil-
 31 ity of the neuron (e.g., see [5,9] making it sensitive to the timing of the stimulus: a
 stimulus can evoke a spike or not depending on how its arrival time is related to the
 33 phase of oscillation.

Injecting sinusoidal currents of different frequency we observe a resonant response,
 35 see Fig 2B. In this simulation, we have added a sinusoidal current of frequency f to

Table 1

This table reports the values of parameters used in the model

Parameters of the model			
Current type	g_{max} , ($\mu\text{S}/\text{cm}^2$)	V_{rev} (mV)	Gating function parameters
<i>Ionic currents</i>			
I_{K-ir}	900	- 84.69	$m_{\infty} = \frac{1}{1 + A_m \exp(-\frac{v - v_{m0}}{k_m})}$ $A_m = 1.28$ $v_{m0} = -83.94 \text{ mV}$
I_{Na-p}	20	- 87.39	$a_{\infty} = \frac{1}{1 + \exp(-\frac{v - v_{a0}}{k_a})}$ $k_m = 14.49 \text{ mV}$ $v_{a0} = -42 \text{ mV}$ $k_a = 5 \text{ mV}$
I_{K-slow}	180	- 84.69	$n_{\infty} = \frac{1}{1 + \exp(-\frac{v - v_{n0}}{k_n})}$ $v_{n0} = -30 \text{ mV}$ $k_n = 6 \text{ mV}$ $\tau_n = \frac{1}{\alpha_n + \beta_n}$ $A_{\alpha n} = 3.3 \text{ s}^{-1}$ $A_{\beta n} = 3.3 \text{ s}^{-1}$ $\alpha_n = A_{\alpha n} \exp((v - v_{\alpha n0})/k_{\alpha n0})$ $v_{\alpha n0} = -30 \text{ mV}$ $\beta_n = A_{\beta n} \exp((v - v_{\beta n0})/k_{\beta n0})$ $k_{\alpha n0} = 40 \text{ mV}$ $v_{\beta n0} = -30 \text{ mV}$ $k_{\beta n0} = -20 \text{ mV}$
I_{LeakA}	56.8	- 58	
I_{GABA-A}	21.7	- 65	
<i>Others parameters: $C = 1 \mu\text{F}/\text{cm}^2$, $V_{th} = -25 \text{ mV}$</i>			

g_{max} is the maximum conductance value used for each current, V_{rev} is the ionic reversal potential and V_{th} is the spiking threshold. The values of parameters are derived from Ref. [5].

1 a weak depolarizing step

$$I_{App} = I_0 + I_1 \sin(2\pi ft),$$

with $I_0 = 2 \text{ pA}$ and $I_1 = 4 \text{ pA}$ in the case shown in Fig 2B., spike bursts are generated in correspondence with the positive phase of the oscillatory current. We measured the spike frequency within the burst as the average interspike intervals between following spikes. The resonance frequency is in the range of 6–10 Hz and in good agreement with experimental observations [4]. Resonant neurons can play an important role in temporal coding; e.g., one can activate selectively a certain neuron sending a burst at its resonant frequency [5].

In conclusion, we have proposed a two-dimensional model of a neuron that is able to capture the main features of a cerebellar granule cell behavior, such as oscillations and resonance. This simplified model can be derived from a multi-dimensional Hodgkin–Huxley neuron introduced in [4]. The use of a low-dimensional model has the advantage of a greater computational efficacy, that allows to implement large scale networks and

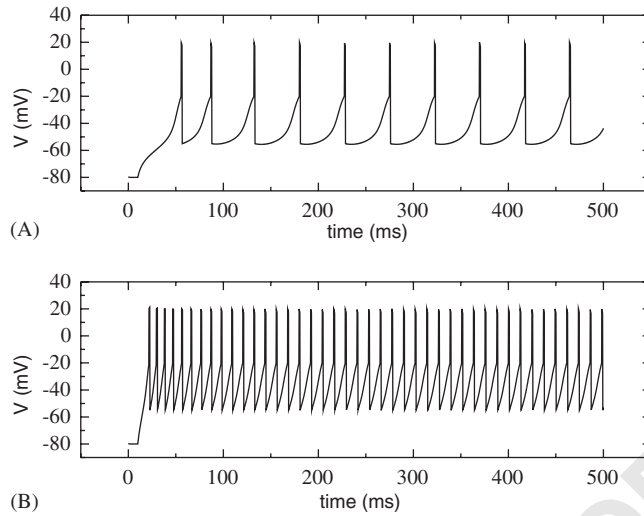


Fig. 1. Current clamp simulations: Two traces are shown: (A) 10 pA, (B) 20 pA.

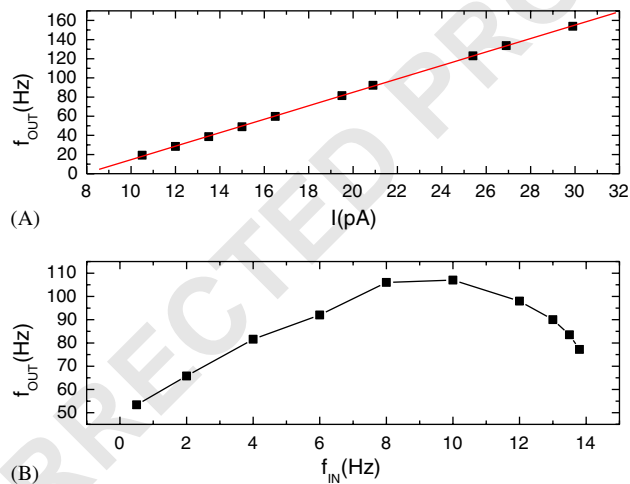


Fig. 2. Excitability properties. (A) The $f-I$ curve show a linear relationship with 7.0 Hz/pA. (B) Resonance is reproduced by a step of 2 pA plus a sinusoidal wave of 4 pA amplitude with variable frequency.

1 of an easier identification of critical elements, sometimes obscured from the many details present in multidimensional models.

3 2. Uncited references

[3,6]

1 **References**

- 3 [1] O.J.-M.D. Coenen, M.P. Arnold, T.J. Sejnowski, M.A. Jabri, Parallel fiber coding in the cerebellum for
life-long learning, *Autonomous Robots* 11 (3) (2001) 291–297.
- 5 [2] E. D’Angelo, G. De Filippi, P. Rossi, V. Taglietti, Synaptic excitation of individual rat cerebellar granule
cells in situ: evidence for the role of NMDA receptors, *J. Physiol. (Lond)* 484 (1995) 397–413.
- 7 [3] E. D’Angelo, G. De Filippi, P. Rossi, V. Taglietti, Ionic mechanism of electroresponsiveness in
cerebellar granule cells implicates the action of a persistent sodium current, *J. Neurophysiol.* 80 (1998)
493–503.
- 9 [4] E. D’Angelo, T. Nieuw, A. Maffei, S. Armano, P. Rossi, V. Taglietti, A. Fontana, G. Naldi,
Theta-frequency bursting and resonance in cerebellar granule cells: experimental evidence and modeling
11 of a slow K^+ -dependent mechanism, *J. Neurosci.* 21 (3) (2001) 759–770.
- [5] E.M. Izhikevich, Resonate-and-fire neurons, *Neural Networks* 14 (2001) 883–894.
- 13 [6] H.J. Jonker, A.C. Coolen, J.J. Denier van der Gon, Autonomous development of decorrelation filters in
neural networks with recurrent inhibition, *Network* 9 (3) (1998) 345–362.
- 15 [7] L. Lapique, Sur L’Excitation Electrique des nerfs, *J. Physiol. (Paris)* 9 (1905) 620–635.
- [8] D. Marr, A theory of the cerebellar cortex, *J. Physiol. (Lond)* 202 (1969) 437–470;
- 17 J.S. Albus, A theory of cerebellar function, *Math. Biosci.* 10 (1971) 25–61.
- [9] M. Richardson, N. Brunel, V. Hakim, From sub-threshold to firing-rate resonance, *J. Neurophysiol.* 89
19 (2003) 2538–2554.
- [10] N. Schweighofer, K. Doya, F. Lay, Unsupervised learning of granule cell sparse codes enhances
21 cerebellar adaptive control, *Neuroscience* 103 (1) (2001) 35–50.
- [11] G.D. Smith, C.L. Cox, S.M. Sherman, J. Rinzel, Fourier analysis of sinusoidally-driven thalamocortical
23 relay neurons and a minimal integrate-and-fire-or-burst model, *J. Neurophysiol.* 83 (1) (2000) 588–610.